Proceedings of the Combustion Institute, Volume 29, 2002/pp. 1559–1564

EFFECT OF VOLUMETRIC HEAT LOSS ON TRIPLE-FLAME PROPAGATION

R. DAOU, J. DAOU AND J. DOLD
Department of Mathematics, UMIST, Manchester M60 1QD, United Kingdom

We present a numerical study of the effect of volumetric heat loss on the propagation of triple flames in the strained mixing layer formed between two opposed streams of fuel and air. The propagation speed of the triple flame is computed for a wide range of values of two non-dimensional parameters: a normalized flame thickness ε, proportional to the square root of the strain rate, and a heat-loss parameter κ. It is shown that, for relatively small values of κ, the propagation speed U is decreased by heat loss, and its dependence on ε is similar to the adiabatic case, known in the literature; in particular, a monotonic decrease in the speed from positive to negative values is observed as ε is increased. However, for κ larger than a critical value, this monotonic behavior is lost. It is shown that the more complex behavior obtained is mainly associated with the fact that, in the presence of heat loss, the trailing planar diffusion flame is extinguished both for sufficiently large and sufficiently small values of the strain rate. Moreover, for sufficiently small values of ε, the dependence of U on κ is similar to that of the non-adiabatic planar premixed flame, with total extinction occurring for a finite positive value of U. On the other hand, for larger values of ε, negative speeds, corresponding to extinction fronts, appear before total extinction is brought about by an increase in κ. A summary of the main results is provided by delimiting the different combustion regimes observed in the κ–ε plane.

Introduction

The importance of triple flames is now well established, in applications involving combustion phenomena, such as flame spread over solid or liquid fuel surfaces, flame propagation in mixing layers, dynamic extinction of diffusion flames, and flame stabilization in reactive streams. Early experimental observation of this structure was made by Phillips [1] and an early analytical description appears in Ohki and Tsuge [2]. Detailed analysis of triple flames and their propagation regimes was undertaken by Dold and collaborators [3,4]. Several aspects of the problem have since been investigated, including the effect of gas expansion, the influence of non-unit Lewis numbers and the stability of triple flames (see Refs. [5–11] and references therein).

The aim of this work is to extend current knowledge of triple flames by taking into account the influence of volumetric heat loss. This aspect of the problem seems to have received no attention, at least as far as the prototypical counterflow configuration is concerned. The aim of this paper is to investigate how triple flames, and their propagation regimes, are affected by volumetric heat loss in this configuration. The paper is structured as follows: the problem is first formulated in the context of a thermo-diffusive approximation, with constant density and constant transport properties and a single Arrhenius reaction; this is followed by presentation and discussion of the numerical findings, in terms of two main parameters related to the strain rate and the rate of heat loss.

Formulation

The study is carried out in the familiar counterflow configuration, illustrated in Fig. 1, with the upper stream carrying oxidizer and the lower stream carrying fuel. The flow components are given by $v_X = 0$, $v_Y = -aY$ and $v_Z = aZ$, in the X,Y, and Z directions, respectively, with a denoting the strain rate. We shall address the steady propagation of triple flames in the mixing layer along the X axis, with the propagation speed $\hat{U}$ being positive if the fronts are moving along the negative X direction. The

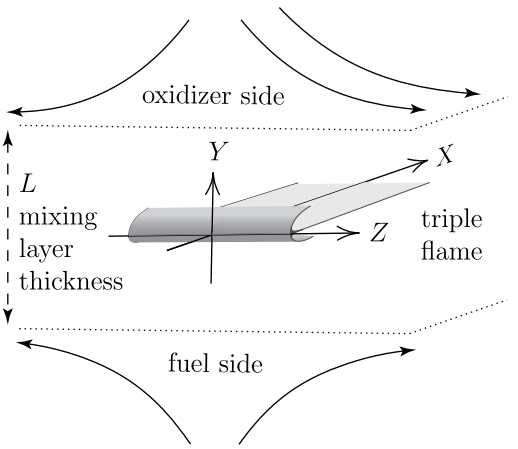

FIG. 1. The counterflow configuration.

chemistry is modeled by a single irreversible one-step reaction of the form $F + s\,Ox \rightarrow P + q$, where F denotes the fuel, Ox the oxidizer, and P the products. The quantities s and q represent the proportion of oxidizer consumed, to fuel consumed, and the heat released per unit mass of fuel. The reaction rate, $\hat{\omega}$, is assumed to follow an Arrhenius law of the form $\hat{\omega} = B\rho^2 Y_F Y_O \exp(-E/RT)$, where B, ρ, Y_F, Y_O, and E/R represent the pre-exponential factor, the (constant) density, the mass fractions of fuel and oxidizer, and the activation temperature, respectively. The stretching of the flow in the Z direction tends to make the system uniform in Z, so that, in a reference frame attached to the flame, the governing equations become

$$\hat{U}\frac{\partial T}{\partial X} = D_T\left(\frac{\partial^2 T}{\partial X^2} + \frac{\partial^2 T}{\partial Y^2}\right) + \frac{q}{c_p}\frac{\hat{\omega}}{\rho} + aY\frac{\partial T}{\partial Y} - \hat{\kappa}(T - T_0) \quad (1)$$

$$\hat{U}\frac{\partial Y_F}{\partial X} = D_F\left(\frac{\partial^2 Y_F}{\partial X^2} + \frac{\partial^2 Y_F}{\partial Y^2}\right) - \frac{\hat{\omega}}{\rho} + aY\frac{\partial Y_F}{\partial Y} \quad (2)$$

$$\hat{U}\frac{\partial Y_O}{\partial X} = D_O\left(\frac{\partial^2 Y_O}{\partial X^2} + \frac{\partial^2 Y_O}{\partial Y^2}\right) - s\frac{\hat{\omega}}{\rho} + aY\frac{\partial Y_O}{\partial Y} \quad (3)$$

Here, D_F, D_O, and D_T are constant diffusion coefficients. The last term on the right of equation 1 is included to account for a linear volumetric heat loss with coefficient $\hat{\kappa}$, the temperature in both incoming streams being T_0. The boundary conditions for equations 1–3, given in non-dimensional form below, correspond to the planar Y-dependent frozen solution as $X \rightarrow -\infty$ or $Y \rightarrow \pm\infty$, and to vanishing X derivatives as $X \rightarrow +\infty$.

The non-dimensional formulation of the problem follows Ref. [9] with the scaled dependent variables being defined by

$$y_F = \frac{Y_F}{Y_{F,st}}, \quad y_O = \frac{Y_O}{Y_{O,st}}, \quad \text{and } \theta = \frac{T - T_0}{T_{ad} - T_0}$$

Here the subscript "st" refers to values at ($X = -\infty$, $Y = Y_{st}$), where Y_{st} is the location of the upstream stoichiometric surface defined by $Y_O = sY_F$, or

$$S\,\mathrm{erf}(Y_{st}/(2D_F/a)^{1/2}) + \mathrm{erf}(Y_{st}/(2D_O/a)^{1/2}) = S - 1$$

with $S \equiv s(Y_F|_{y=\infty})/(Y_O|_{y=-\infty})$. The quantity T_{ad} is defined by $T_{ad} \equiv T_0 + qY_{F,st}/C_p$. As unit length, we select L/β, where $L \equiv (2D_T/a)^{1/2}$ is the (thermal) mixing layer thickness and $\beta \equiv E(T_{ad} - T_0)/RT_{ad}^2$ is the Zeldovich number; the unit of length is then a typical radius of curvature of a triple flame. As unit speed, we adopt the laminar speed of a stoichiometric planar flame, or more precisely its asymptotic value for large β under adiabatic equidiffusional conditions, namely $S_L^0 = (4\beta^{-3}Y_{O,st}\rho D_T B \exp(-E/RT_{ad}))^{1/2}$.

In terms of the coordinates $y \equiv \beta(Y - Y_{st})/L$ and $x \equiv \beta X/L$, equations 1–3 now assume the non-dimensional form

$$U\frac{\partial\theta}{\partial x} = \varepsilon\left(\frac{\partial^2\theta}{\partial x^2} + \frac{\partial^2\theta}{\partial y^2}\right) + \varepsilon^{-1}\omega + \frac{2\varepsilon}{\beta}\left(\eta_s + \frac{y}{\beta}\right)\frac{\partial\theta}{\partial y} - \frac{\varepsilon^{-1}}{\beta}\kappa\theta \quad (4)$$

$$U\frac{\partial y_F}{\partial x} = \frac{\varepsilon}{Le_F}\left(\frac{\partial^2 y_F}{\partial x^2} + \frac{\partial^2 y_F}{\partial y^2}\right) - \varepsilon^{-1}\omega + \frac{2\varepsilon}{\beta}\left(\eta_s + \frac{y}{\beta}\right)\frac{\partial y_F}{\partial y} \quad (5)$$

$$U\frac{\partial y_O}{\partial x} = \frac{\varepsilon}{Le_O}\left(\frac{\partial^2 y_O}{\partial x^2} + \frac{\partial^2 y_O}{\partial y^2}\right) - \varepsilon^{-1}\omega + \frac{2\varepsilon}{\beta}\left(\eta_s + \frac{y}{\beta}\right)\frac{\partial y_O}{\partial y} \quad (6)$$

Here, the parameter ε, the square of which is the inverse of the Damköhler number, is defined by

$$\varepsilon \equiv \frac{l_{Fl}^0}{L/\beta} \equiv \frac{\beta(D_T/2)^{1/2}}{S_L^0}\,a^{1/2}$$

It represents the thickness of the laminar stoichiometric flame $l_{Fl}^0 = D_T/S_L^0$, measured in terms of our standard unit of length L/β. The Lewis numbers of fuel and oxidizer are $Le_F \equiv D_T/D_F$ and $Le_O \equiv D_T/D_O$, and $\eta_s \equiv Y_{st}/(2D_T/a)^{1/2}$ characterizes the location of the upstream stoichiometric surface. The non-dimensional heat loss coefficient is $\kappa \equiv \beta(D_T/S_L^{02})\hat{\kappa}$ and ω is given by

$$\omega \equiv \frac{\beta^3}{4}\,y_F\,y_O\exp\left(\frac{\beta(\theta - 1)}{1 + \alpha(\theta - 1)}\right) \quad (7)$$

with $\alpha \equiv (T_{ad} - T_0)/T_{ad}$.

In terms of the new variables, the boundary conditions as $x \rightarrow -\infty$ or $y \rightarrow \pm\infty$ are

$$\theta = 0$$

$$y_F = \frac{1 - \mathrm{erf}[(\eta_s + y/\beta)Le_F^{1/2}]}{1 - \mathrm{erf}(\eta_s Le_F^{1/2})}$$

$$y_O = \frac{1 + \mathrm{erf}((\eta_s + y/\beta)Le_O^{1/2})}{1 + \mathrm{erf}(\eta_s Le_O^{1/2})} \quad (8)$$

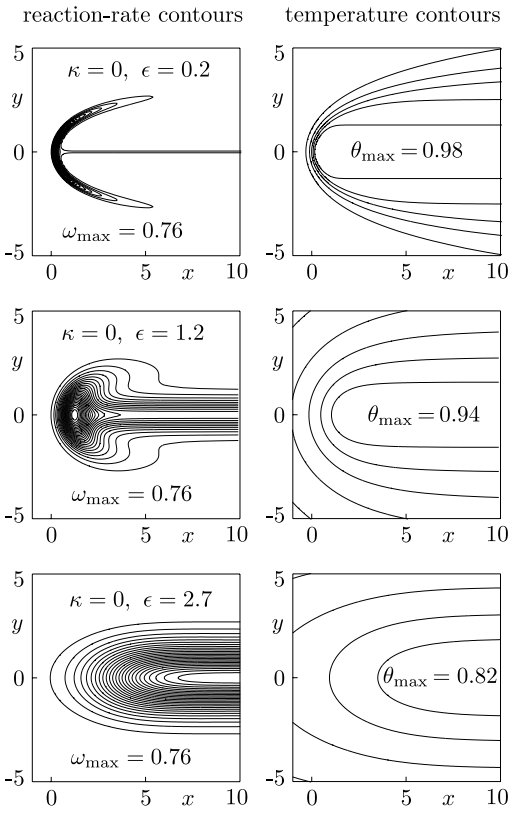

FIG. 2. Contours of the reaction rate (left) and temperature (right) for the cases $\kappa = 0$ with $\varepsilon = 0.2$ (top), $\varepsilon = 1.2$ (middle), and $\varepsilon = 2.7$ (bottom).

and as $x \to +\infty$

$$\frac{\partial \theta}{\partial x} = \frac{\partial y_F}{\partial x} = \frac{\partial y_O}{\partial x} = 0 \qquad (9)$$

In solving this problem, the main aim is to determine the (scaled) propagation speed U in terms of the non-dimensional parameters ε, κ, Le_F, Le_O, and η_s (as well as β and α). In this study, we provide detailed numerical results in terms of the parameters ε and κ.

Results

The problem consisting of equations 4–6 with the boundary conditions 8 and 9 is solved numerically. The numerical method is the same as the one used in Ref. [9] and is based on a finite volume discretization combined with an algebraic multigrid solver [12]. The computational domain dimensions are typically 10 times the mixing layer thickness in the y direction and 100 times the planar laminar flame thickness in the x direction. The grid is non-uniform with typically 200,000 points. We report results describing the dependence on the parameters ε and κ, with the other parameters being assigned fixed values, namely $\beta = 8$, $\alpha = 0.85$, $\eta_s = 0$, and $Le_F = Le_O = 1$.

We begin by presenting a reference case corresponding to the familiar adiabatic situation $\kappa = 0$. Shown in Fig. 2 are reaction rate contours (left) and corresponding temperature contours (right). The subfigures correspond to $\varepsilon = 0.2$, 1.2, and 2.7, from top to bottom, with the last value characterizing near-extinction conditions. The contours are equidistributed between zero and the maximum value of the field, which is indicated in each subfigure. The dimensionless leading front becomes thicker for larger values of ε (or strain rate) which is accompanied by a decrease in the propagation speed from positive to negative values (see Fig. 4). Of course, in the limit $\varepsilon \to 0$, corresponding to large Damköhler numbers, the temperature of the trailing diffusion flame increases to unity, its adiabatic value, while the corresponding reaction rate ω decreases to zero (due to a vanishing rate of supply of the reactants to the reaction zone); as ε is increased this trend is reversed, at least up to near-extinction conditions (obtained for sufficiently high strain rates).

To illustrate the influence of heat loss on the triple flame, Fig. 3 depicts the same situation as Fig. 2, with $\kappa = 0.04$, for $\varepsilon = 0.2$, 1.2, and 2.4; the final value again characterizes near-extinction conditions and is smaller than in the adiabatic case. An important feature associated with the presence of heat loss is the extinction of the trailing diffusion flame for small values of ε, as can be observed in the top subfigures. Otherwise, the behavior of the triple flame as ε is increased is similar to the adiabatic case, with the fronts evolving continuously from propagating fronts to retreating fronts until total extinction occurs.

However, it is important to note that the last remark is valid only for sufficiently small values of κ. For κ larger than some critical value, more complex behavior is obtained. This is best illustrated by plotting the propagation speed U versus ε for selected values of κ, as done in Fig. 4. The curve labeled $\kappa = 0$ in this figure is the well-known adiabatic case. This curve has a vertical slope for a critical value of ε which characterizes the total extinction of the triple-flame structure. As explained in Ref. [13], this critical value is associated with the quenching of the planar diffusion flame by an excessively high strain rate. We note that the curve labeled $\kappa = 0.04$ displays a similar trend, in line with the observations above, but that the cases corresponding to higher values of κ exhibit a markedly different behavior. In particular, the dependence of U on ε is no longer monotonic and, in fact, the ε-domain of existence of the flame fronts separates into two disjoint intervals; this is clearly seen in the curves corresponding to $\kappa = 0.05$ and 0.06. For yet larger values of κ, no

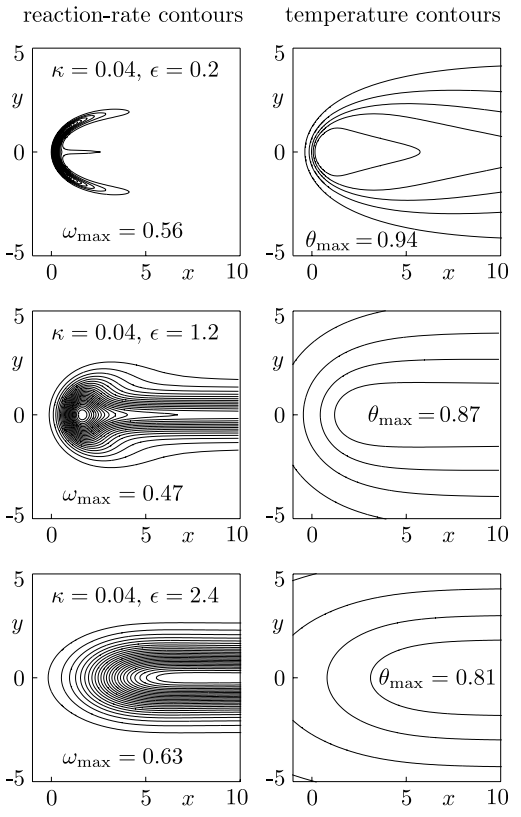

FIG. 3. Contours of the reaction rate (left) and temperature (right) for the cases $\kappa = 0.04$ with $\varepsilon = 0.2$ (top), $\varepsilon = 1.2$ (middle), and $\varepsilon = 2.4$ (bottom).

solutions are found for small values of ε, as seen in the curve for $\kappa = 0.08$. This can be explained by the fact that, as $\varepsilon \to 0$, the propagation speed tends to that of the stoichiometric planar flame, but the latter ceases to exist for excessive heat losses even though a narrower flame edge can still exist at higher values of ε (according to numerical experiments). For larger values of κ, approximately $\kappa > 0.1$ in this example, we found no burning solutions for any value of ε.

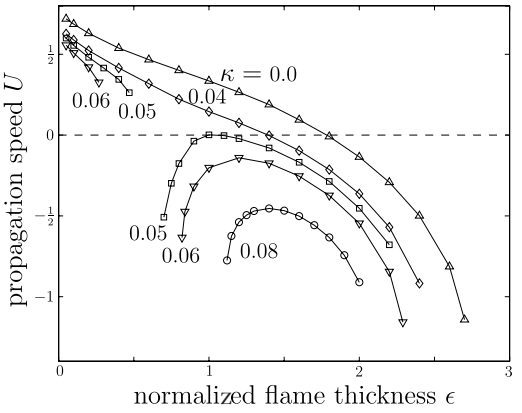

FIG. 4. Plots of U versus ε for selected values of κ.

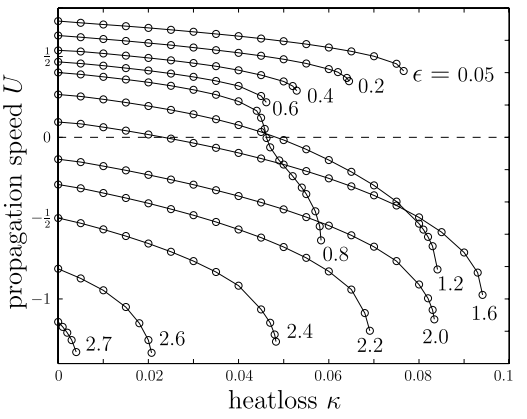

FIG. 5. Plots of U versus κ for selected values of ε.

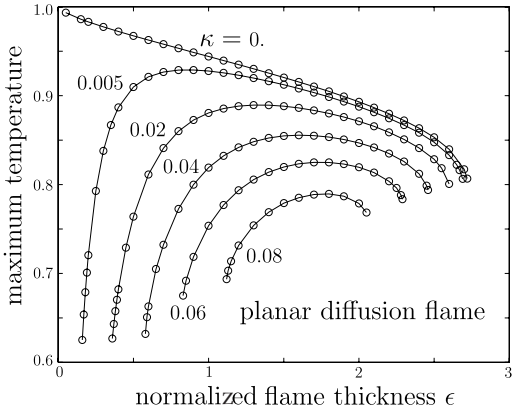

FIG. 6. Maximum temperature versus ε for selected values of κ for the planar diffusion flame.

Another instructive way of examining the results just presented is to plot U versus κ for selected values of ε, as in Fig. 5. For small values of ε, the dependence of U on κ is similar to that of the nonadiabatic planar flame, with extinction occurring at a finite positive speed. This can be confirmed by an asymptotic analysis in the limit $\varepsilon \to 0$, which is not included here due to space limitations. From the figure, we can also conclude that retreating triple flames (or extinction fronts, having $U < 0$) can be obtained by increasing the intensity of the heat loss only if ε (or the strain rate) is above a critical value.

To understand better the dependence of U on ε, in the presence of heat loss, it is useful to compare it with a numerical description of the planar

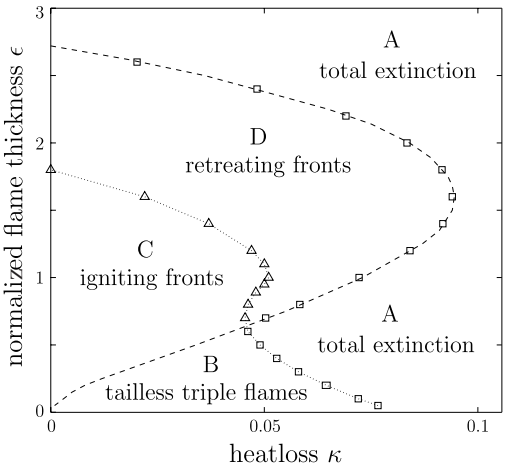

FIG. 7. Regimes of triple-flame propagation, with and without an associated diffusion flame, in the presence of heat loss.

diffusion flame over the same ranges of parameters. The latter is presented in Fig. 6, where the maximum temperature of the planar diffusion flame is plotted against ε for several values of κ. We note that for any non-zero value of κ, there are two extinction values of ε, a fact that is known in the literature (see, for example, Refs. [14–17]). The larger extinction limit, which is also encountered in the adiabatic case, is due to flame quenching by an excessively high strain rate. The lower extinction limit is partly associated with the fact that the rate of heat generation by the chemical reaction decreases as the strain rate (or reactant supply) is decreased, leading to extinction for any non-zero value of κ; moreover, the total size of the region of hot gas also increases, which increases the total heat loss and lowers the flame temperature. The fact that extinction must occur can be seen from the following simple, order-of-magnitude argument.

From the diffusive-reactive balance in the thin reaction zone, of typical (non-dimensional) thickness δ_r, say, we have from the one-dimensional y-dependent version of equations 5 and 6

$$\frac{\bar{y}_F}{\delta_r^2} \sim \frac{\bar{y}_O}{\delta_r^2} \sim \varepsilon^{-2}\bar{\omega}$$

where the bars indicate typical values in the reaction zone. From equation 7, supposing that $\bar{\theta}$ is close to unity

$$\bar{\omega} \sim \beta^3 \bar{y}_F \bar{y}_O$$

Since the order of magnitude of the gradients of y_F and y_O in the reaction zone, $\bar{y}_F/\delta_r$ and $\bar{y}_O/\delta_r$, respectively, are the same as in the mixing layer (whose non-dimensional thickness is β, given our choice of unit length) we may write

$$\frac{\bar{y}_F}{\delta_r} \sim \frac{\bar{y}_O}{\delta_r} \sim \frac{1}{\beta}$$

From the last three equations, it follows that $\delta_r \sim \beta^{-2/3}\varepsilon^{2/3}$, and

$$\bar{\omega} \sim \beta^{-1/3}\varepsilon^{4/3}$$

Now, using the temperature equation 4, we see that the effective rate of heat generation (accounting for heat loss) is given, in order of magnitude, by $\bar{\omega} - \kappa/\beta$. This quantity becomes negative in the limit $\varepsilon \to 0$, indicating that the temperature decreases, leading to extinction, whenever $\kappa > 0$. It also indicates that extinction must occur at least when $\kappa = O(\beta^{2/3}\varepsilon^{4/3})$, or larger. For the adiabatic case, $\kappa = 0$, extinction is impossible as $\varepsilon \to 0$, since the net rate of heat generation remains positive, although it becomes vanishingly small. This is the classical Burke–Schumann limit.

We now return to Figs. 4 and 6, where it is seen, by comparing, for example, the curves labeled $\kappa = 0.06$, that the more complex dependence of U on ε when $\kappa \neq 0$ is directly linked to the behavior of the planar diffusion flame. This explains, when κ is not too small, both the monotonic variation of U with ε and the fact that the ε-domain of existence of the flame fronts consists of two disjoint intervals. For small values of κ, for example $\kappa = 0.04$, the lower extinction limit of the diffusion flame occurs at values of ε, which are sufficiently small to have a negligible effect on the propagation speed. This is because, for sufficiently small values of ε, the leading premixed front is negligibly affected by the properties of the fields downstream, and hence by the trailing diffusion flame.

Finally, a summary of the main results is presented in Fig. 7 in the space of κ and ε. The dashed line characterizes the extinction limits of the planar diffusion flame extracted from the previous figure. The squares correspond to the complete extinction of the triple-flame structure, and are (partially) extracted from Fig. 5. The triangles describe conditions with zero-propagation speeds. Four combustion regimes can thus be delimited in the κ–ε plane.

1. In the domain labeled A, to the right of the squares, the triple-flame structure is extinguished. We note that the extinction in this case is dictated by the extinction of the diffusion flame in situations where the squares lie on the dashed line. This occurs for ε larger than a critical value ε^* which is seen to be close to 0.7. For small values of the strain rate (more precisely for $\varepsilon < \varepsilon^*$), the triple-flame structure survives in situations where the planar diffusion flame is extinguished.
2. In the domain labeled B, to the left of the squares and below the lower branch of the dashed curve, the triple flames have positive speeds and no trailing diffusion-flame tail (far downstream), as

exemplified in the top subfigure of Fig. 3. We could call these tailless triple flames. More generally, such structures arise in situations where the flame behind a flame edge is extinguished but the edge itself continues to survive. Such structures share some similarities with those encountered in low Lewis number triple-flame studies (see Ref. [18]) where oscillatory propagation arises.

3. In domain C, below the triangles and above domain B, triple flames with positive speeds and trailing diffusion-flame tails are encountered. These may be referred to as ignition fronts of the diffusion flame, as in the familiar adiabatic situation.
4. In the remaining domain, D, negatively propagating triple flames (retreating fronts) are obtained, again as found in the adiabatic situation.

Conclusion

We have presented a numerical description of triple-flame propagation in a strained mixing layer under nonadiabatic conditions. The results indicate that various combustion regimes arise, due to the difference in sensitivity to heat loss of the premixed leading front and trailing diffusion flame. In particular, a synthesis of the main findings has been given in terms of the heat-loss intensity and the strain rate. It is worth pointing out that the solutions presented have been obtained by solving the steady-state-governing equations. Their stability, which has not been addressed in this work, will be checked in future studies by solving the corresponding time-dependent problem.

Acknowledgment

The authors are grateful to the EPSRC for financial support.

REFERENCES

1. Phillips, H., *Proc. Combust. Inst.* 10:1277 (1964).
2. Ohki, Y., and Tsuge, S., in *Dynamics of Reactive Systems, Part I* (J. R. Bowen, J. C. Leyer, and R. I. Soloukhin, eds.), Progress in Astronautics and Aeronautics, 1986.
3. Dold, J. W., *Combust. Flame* 76:71–88 (1989).
4. Hartley, L. J., and Dold, J. W., *Combust. Sci. Technol.* 80:23 (1991).
5. Liñán, A., in *Combustion in High Speed Flows* (J. Buckmaster, T. L. Jackson, and A. Kumar, eds.), Kluwer Academic, Boston, 1994, p. 461.
6. Kioni, P. N., Rogg, B., Bray, C., and Liñán A., *Combust. Flame* 95:276–290 (1993).
7. Buckmaster, J., and Matalon, M., *Proc. Combust. Inst.* 22:1527–1535 (1988).
8. Ruetsch, G. R., Vervisch, L., and Liñán, A., *Phys. Fluids* 7(6): (1995).
9. Daou, J., and Liñán, A., *Combust. Theory Model.* 2:449–477 (1998).
10. Shay, M. L., and Ronney, P. D., *Combust. Flame* 112:171 (1998).
11. Short, M., Buckmaster, J., and Kochevets, S., *Combust. Flame* 125:893 (2001).
12. Ruge, J., and Stüben, K., in *Proceedings of Multigrid Conference,* Bristol, 1983.
13. Dold, J. W., *Prog. Astronaut. Aeronaut.* 173:61–72 (1997).
14. Sohrab, S. H., Liñán, A., and Williams, F. A., *Combust. Sci. Technol.* 27:143–154 (1982).
15. Liu, F., Smallwood, G. J., Gülder, Ö. L., and Ju, Y., *Combust. Flame* 121:275–287 (2000).
16. T'ien, J. S., *Combust. Flame* 65:31–34 (1982).
17. Chao, B. H., Law, C. K., and T'ien, J. S., *Proc. Combust. Inst.* 23:523 (1990).
18. Thatcher, R. W., and Dold, J. W., *Combust. Theory Model.* 4:435–457 (2000).

COMMENTS

Ishwar K. Puri, University of Illinois at Chicago, USA. I applaud your motivation; your results are intuitive and some are well known, namely, reduction in flame propagation speed with heat loss and extinction, and the formation of a flame nub with increasing stretch. However, I have some reservation. You assume a uniform global volumetric heat loss, whereas a real radiating flame would lose heat according to its non-uniform product distribution. Further, whereas you have assumed a constant strain rate, a realistic flame experiences non-uniform stretch along its topology that depends on flame curvature, hydrodynamic straining, and flame thickness.

Author's Reply. The objective of the article is to establish qualitative rather than quantitative accuracy in describing the effect of heat loss on strained triple flames. This is as much as can be expected when, for example, using a one-step model for the chemistry. For this purpose, using a simple model has numerous advantages. A more sophisticated model could certainly be adopted, and the likelihood is that exactly the same forms of behavior would be observed, differing only in detail. The model adopted here, including that for heat loss, is chosen to fit in with other studies which, for example, have indeed shown a reduction in the flame speed of a planar premixed flame with heat loss, as you say. However, we are aware of no existing analytical or numerical studies that describe the combination of phenomena that we have observed, including the appearance of a tailless propagating flame edge. We have recently submitted another article that examines the phenomena from a more analytical perspective, which is most easily done using a simple linear model for global heat loss.